

## Electromagnetic Characterization of Recyclable Polymer Nanofibers Based on PSU/Carbonyl Iron

Daniel Cônsoli Silveira<sup>1,\*</sup>, Tiago Teixeira da Silva Braga<sup>1</sup>, Daniel Molina Gil<sup>1</sup>, Newton Adriano dos Santos Gomes<sup>2</sup>, Lilia Müller Guerrini<sup>3</sup> and Edson Cocchieri Botelho<sup>1</sup>

<sup>1</sup>Department of Materials and Technology, São Paulo State University (UNESP), School of Engineering, Guaratinguetá/SP-Brazil.

<sup>2</sup>Electronic Warfare Laboratory, Technological Institute of Aeronautics (ITA), São José dos Campos/SP-Brazil.

<sup>3</sup>Institute of Science and Technology, Federal University of São Paulo (UNIFESP), São José dos Campos/SP-Brazil.

\*Corresponding Author: Daniel Cônsoli Silveira. Email: danielsilveira.tech@gmail.com.

**Abstract:** This study investigated and defined the optimal processing parameters for the electrospinning of polysulfone polymer solutions with N,N-dimethylacetamide. Variation of parameters such as solute concentration, electrical voltage, and working distance were correlated with the quality of the obtained nanofibers using morphological characterization via scanning electron microscopy (SEM). Carbonyl iron additive was dispersed in the polymer solutions, using ultrasonic tip, and the material processed via electrospinning with aforementioned parameters defined. Nanofibers with the property of interaction with electromagnetic waves were obtained. The dispersion of different concentrations of the additive and electromagnetic characterizations in the X-band of microwaves (8.2 and 12.4 GHz), using vector network analyzer (VNA) and rectangular waveguide, allowed the identification of the materials electromagnetic behaviors. Scattering parameters allowed the calculation of reflected and transmitted energy by the material.

**Keywords:** Carbonyl iron; electromagnetic characterization; electrospinning; nanofibers; polysulfone.

### 1 Introduction

The field of nanocomposites is considered one of the most popular, with researches and developments in basically all the technical disciplines. Fundamentally, nanocomposites are composites in which at least one of their phases has a nanometric scale, below 100 nm. Nanocomposites can be classified according to their matrix: ceramic, metallic or polymeric and are high performance materials that exhibit an unusual combination of properties and different forms of presentation [3,4]. Due to its versatility, many applications can be found for nanocomposites. It is important to highlight the advances in engineering with structural materials [5], electronic equipment and systems [6], sensors [7], energy storage [8], biomedicine, with drug delivery [9] and structures of bones, tissues and cartilages [10].

Electrospinning is recognized as an efficient technique in the manufacture of continuous fibers at nanometric scale from various types of polymers, such as natural, synthetic, blends and charged with nanoparticles or additives [11,12]. The technique basically consists on the application of electric field, generated by a voltage source, on the surface of a polymeric solution in a pipette or needle. When the electrical voltage exceeds the polymer solution surface tension, an electrically charged jet of the polymer solution is created, with the evaporation of the solvent before the jet reaches a grounded collector, creating different nanofibers according to applied processing parameters, as well as complexly structured fibers, such as hollow or core-shell fibers by means of specific methods [12,13].

The main fields of application of the nanofibers currently aim medical prostheses [14], filtration systems [15], aerospace composites [16], tissue models [17], liquid crystal devices [18] and electromagnetic shielding [19].

Electromagnetic shielding has become more and more necessary due to the great popularization of electronics and telecommunication systems, becoming intrinsically necessary for components protection [20,21]. The malfunctioning of specific systems can lead to catastrophic failures of different types of equipment, especially those of strategic interest such as aircraft, nuclear reactors, transformers and control/communication systems [21].

The depreciation of electromagnetic interference can be reached through three different methods of interaction with the microwaves. The first consists of the reflection of the microwave, being required the presence of mobile charges that will interact with the electromagnetic field. The second is the absorption of the microwave, which occurs through Joule effect, with the conversion of the electromagnetic energy into heat, being required the presence of electric or magnetic dipoles for the interaction with the electromagnetic fields. The third mechanism occurs due to multiple reflections of the microwave in several interfaces of material, being required the presence of a large surface area [22,23]. The microwave absorption is intrinsically related to the thickness of the material and is usually expressed in decibel (dB) [23].

Most of the polymer matrices do not exhibit microwave absorption properties, however, there are additives that when dispersed in the matrix causes functionalization of resulting material, allowing interaction with microwaves, for instance, metallic fibers, metallic particulates, carbon black and carbon fiber [24]. The matrix used in this study, polysulfone (PSU), is an amorphous thermoplastic renewable polymer [25], intrinsically with no interaction with the microwaves in the X-band. However, with the addition of carbonyl iron, magnetic metallic material that exhibits shielding properties [26], the result is a composite with potential use as electromagnetic interference (EMI) shielding material.

Therefore, the objective of this study is the obtaining, via electrospinning, of nanofibers based on PSU/Carbonyl iron with EMI shielding properties, understanding the respective portions of reflected and transmitted energy by the material.

## **2 Experimental**

### **2.1 Materials**

The polymer solutions prepared used the polysulfone amorphous polymer in the form of pellets with 1.24 g/cm<sup>3</sup> specific mass, 70.3 MPa tensile strength, 2482 MPa tensile modulus, 106.2 MPa flexural strength, 2689 MPa flexural modulus and 185°C glass transition temperature. The organic solvent N,N-Dimethylacetamide, with chemical formula CH<sub>3</sub>CON(CH<sub>3</sub>)<sub>2</sub>, presents specific mass of 0.94 g/cm<sup>3</sup>, 87.12 g/mol molar mass, 165.5°C boiling point, -20°C solidification point, 70°C flash point and 490.3°C ignition point. Finally, the ferromagnetic additive carbonyl iron was supplied by BASF in spherical particles with diameters between 3 and 20 μm and specific mass of 7.8 g/cm<sup>3</sup>.

### **2.2 Processing Parameters**

For the determination of the optimal electrospinning parameters, being polymer concentration, applied electrical voltage and working distance, several blankets were produced with a variety of configurations.

The polymer concentration used was defined as a function of the formation of nanofibers. The proportions used were 8, 12, 20, 26 and 28 %m/m.

The optimized electrospinning parameters were determined by correlation with SEM of the blankets produced using different parameters combinations, with the electrical voltage varying in 15, 18 and 20 kV and working distance (needle tip to top of a cylindrical collector) of 5, 10 and 15 cm.

### **2.3 Nanofibers Production**

The polymer solutions of PSU and N,N-Dimethylacetamide (DMAc) were prepared in a water bath at 70°C and with constant moderate stirring.

The dispersions of carbonyl iron in the solutions were carried out in different concentrations: 3, 5, 8 and 13 %m/m. An ultrasonic tip from Sonics & Materials, model VC 750 was used and sonication was performed for a total of three minutes, intercalating 30 seconds in operation and 10 seconds in standby, to avoid solvent losses, using 50% of the amplitude limit (20 kHz, 750 W).

The electrospinning system consists of a 20 ml Hamilton type syringe connected to a high voltage source, positioned above a grounded rotating collector cylinder with the rotation of 27 rpm. Processing was performed at room temperature and controlled humidity at 50%.

### **2.4 Characterization**

The morphological characterization was performed with a scanning electron microscope (SEM) ZEISS-EVO series model LS15.

Electromagnetic characterization of samples were performed in X-band frequencies of microwaves, from 8.2 to 12.4 GHz. Scattering parameters (transmission and reflection of microwaves) were obtained using an Agilent Technologies vector network analyzer (VNA) model PNA-L N5230C, with four signal generation/capture ports, the ports being used two to two, equipped with frequency generator between 300 kHz and 20 GHz and rectangular waveguide and connectors model 00281-60016 OPTION 006, also from Agilent Technologies.

The samples size in the rectangular waveguide is 10 mm × 22.62 mm, electromagnetic characterizations performed with only one layer of each of the blankets. For the measurements of the scattering parameter, was used port 4 for the reflection measurements and ports 2 and 4 for the transmission measurements.

## **3 Results**

### **3.1 Processing Parameters**

The electrospinning processing parameters were defined in two steps. The first consisted of defining the range of polymer concentration in which nanofibers were formed.

With the aid of SEM, it was not identified the formation of nanofibers with polymer concentrations lower than 26 %m/m and with all configurations of electrical voltage and working distance from this study. The maximum concentration was defined from the viscosity of the solution, with values above 28 %m/m of PSU the solution became excessively viscous, clogging the needle and making it impossible to process.

The second step consisted of the analysis of the quality of the fibers, aiming generation of nanofibers using 26 and 28 %m/m, with the variation of the applied voltage and working distance. In general, it was observed an increase in quality associated with the increase of both applied voltage and working distance, due to the homogeneity and the lower presence of defects.

The optimal parameters were fixed for the concentrations of 26 %m and 28 %m, being respectively 18 kV, 10 cm and 20 kV, 10 cm. The combination was chosen due to greater homogeneity of fiber diameter and fewer defects in the blanket. However, the 26 %m/m PSU concentration presented fibers in micrometric size, while the 28 %m/m PSU concentration presented only fibers in nanometric size. Thus, the optimal parameters were defined as 28 %m/m PSU, 20 kV of applied voltage and 10 cm of working distance. Fig. 1 shows the SEM images of blankets generated.

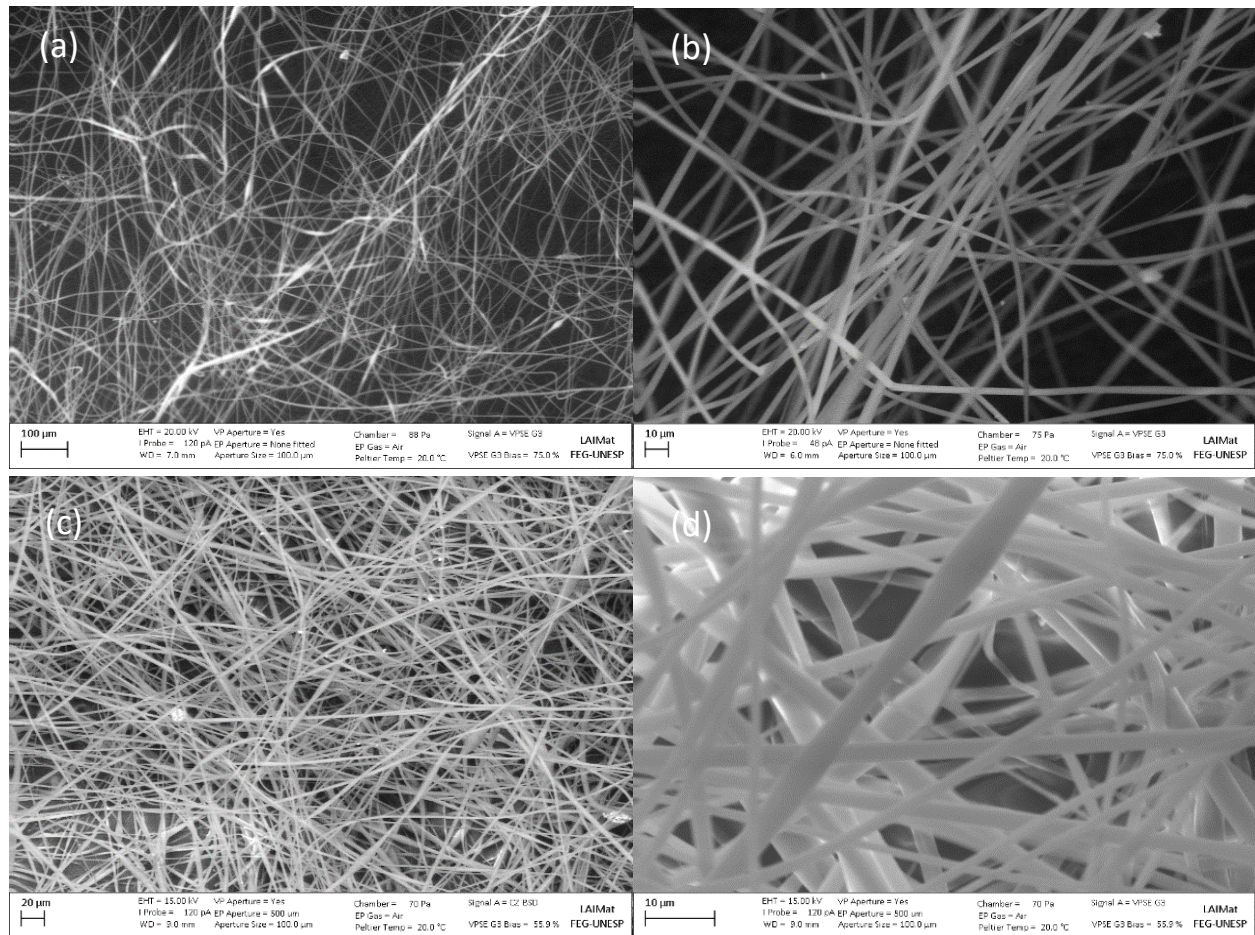


**Figure 1:** SEM of the PSU nanofibers obtained with 28 %m/m PSU, 20 kV and 10 cm [a. 500x, b. 1000x] and 26 %m/m PSU, 18 kV and 10 cm [c. 500x, d. 3000x]

### 3.2 Nanofibers Morphology

The determination of the optimal processing parameters allowed the production of the nanofibers with the best quality. The next step was the dispersion of carbonyl iron, carried out in different concentrations in polysulfone polymer solutions. Concentrations of 3, 5, 8 and 13 %m were used, above these values it became difficult to adequately disperse the additive and when placed in the electrospinning system, the needle clogging occurred due to high viscosity and density with the incorporation of the ferromagnetic additive, making it impossible to process the nanofibers. It is also observed that the increase of the additive concentration promotes the increase in defects of the nanofibers. Fig. 2 shows the SEM of the blankets generated with each carbonyl iron concentration.

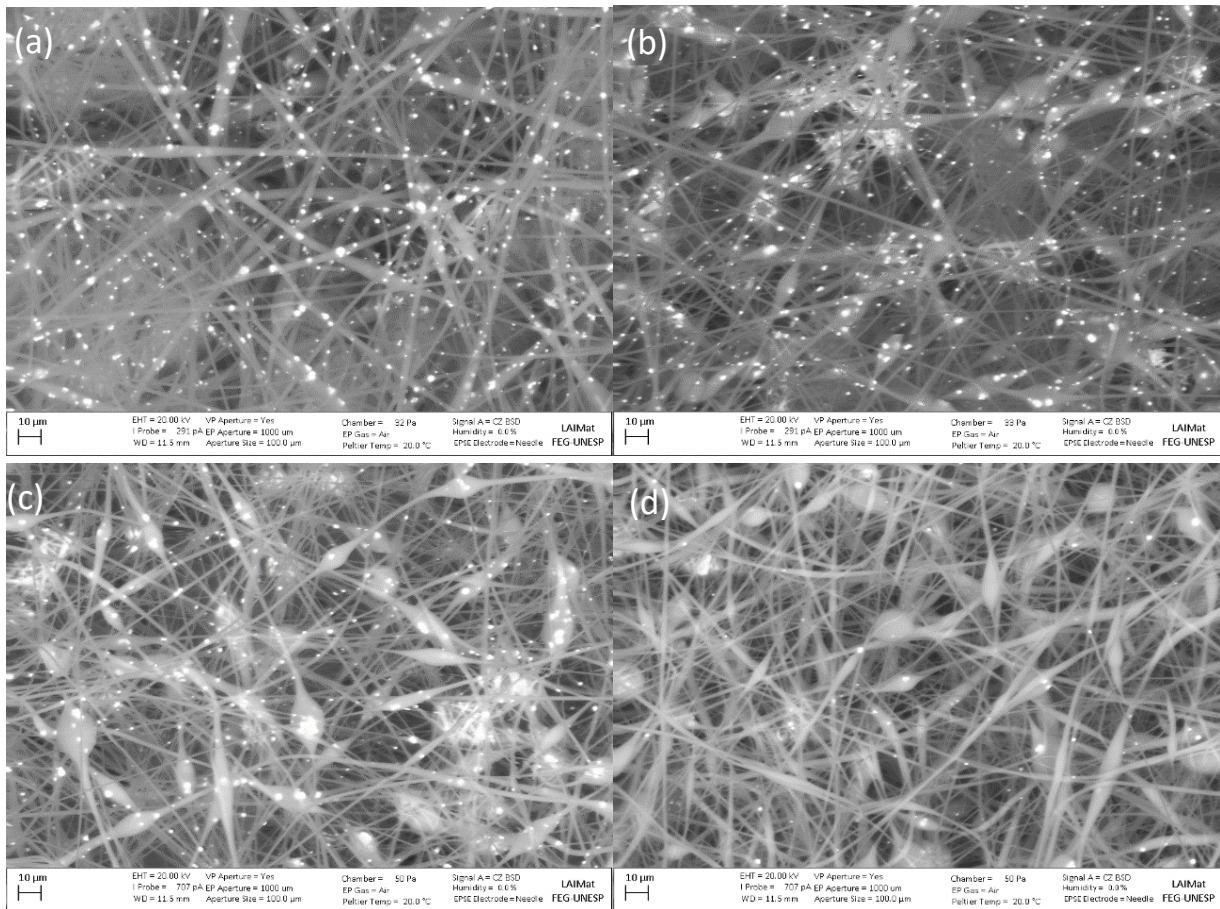


**Figure 2:** SEM of the PSU nanofibers with carbonyl iron obtained with 28 % m/m PSU, 20 kV and 10 cm (1000x) [a. 3 % m/m of carbonyl iron, b. 5 %, c. 8 %, d. 13 %]

### 3.3 Electromagnetic Characterization

After the electrospinning of the blankets with different concentrations of carbonyl iron, the electromagnetic characterization occurred as previously described. Fig. 3 shows the overall performance of the nanocomposites in the evaluated range of 8.2 to 12.4 GHz. Data are plotted as a function of the attenuation, in decibel (dB), at each frequency.

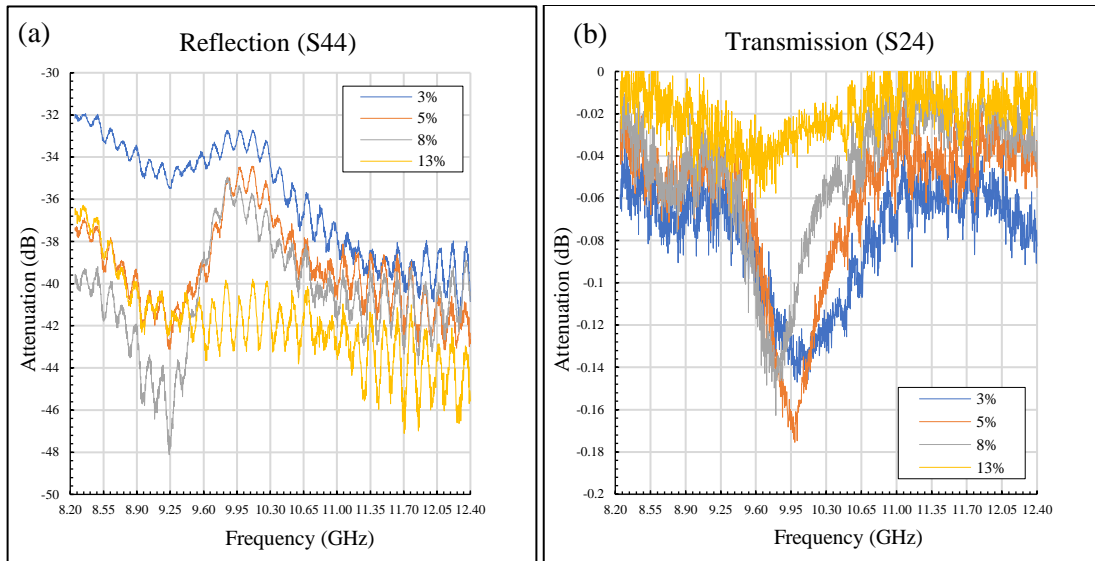


**Figure 3:** Scattering parameters for each percentage of carbonyl iron mass [a. S44 reflection, b. S24 transmission]

Through the electromagnetic characterization results above and equation 1 [27], it is possible to express the data as a function of the percentage of energy reflected and transmitted at each frequency. Results are presented in Fig. 4.

$$\text{Energy gain/loss (\%)} = 100 \cdot \left[ 1 - 10^{\left(\frac{-dB}{10}\right)} \right] \quad (1)$$

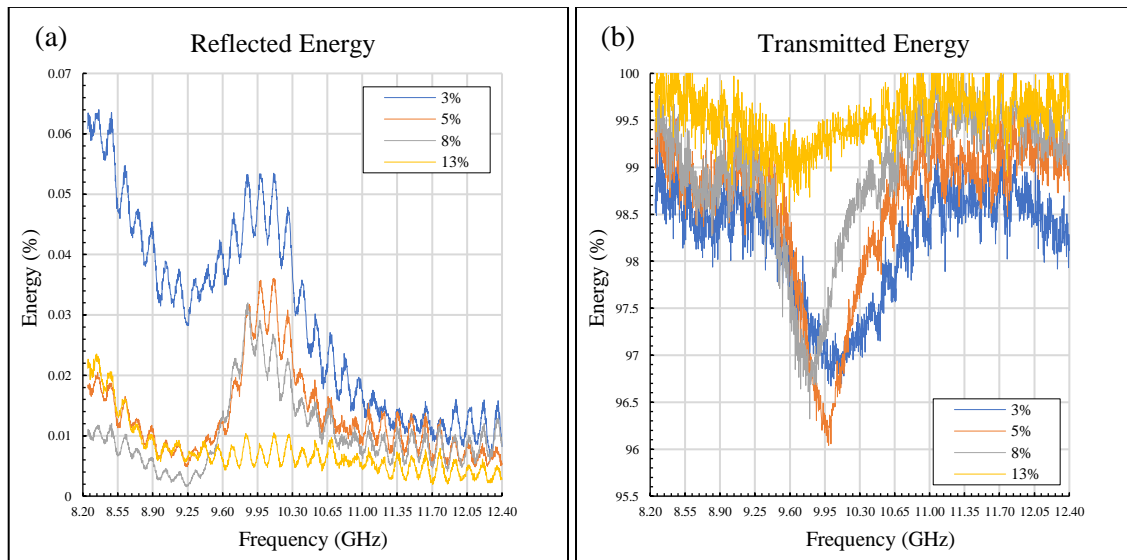


**Figure 4:** Energy portions (%) for each percentage of carbonyl iron %m/m. [a. Reflect Energy, b. Transmitted Energy]

From the comparison of the scattering parameters and the reflected and transmitted energy results, it is observed that the nanofibers have virtually identical behavior, presenting high transmission, low reflection and basically zero absorption.

To evaluate the data, Tab. 1 was prepared, so the results presented above are divided into smaller intervals using mean values.

**Table 1:** Average scattering parameters and percentage of reflected and transmitted energy for each carbonyl iron concentration in frequency ranges

CI Conc. (%m/m)	Range (GHz)	S <sub>44</sub> (dB)	S <sub>24</sub> (dB)	Reflected Energy (%)	Transmitted Energy (%)
<b>3</b>	8.2 to 8.9	32.90	0.062	0.051	98.58
	8.9 to 9.6	34.57	0.069	0.035	98.43
	9.6 to 10.3	33.51	0.122	0.045	97.22
	10.3 to 11	36.43	0.092	0.023	97.90
	11 to 11.7	38.83	0.059	0.013	98.64
	11.7 to 12.4	39.55	0.064	0.011	98.53
<b>5</b>	8.2 to 8.9	38.53	0.046	0.014	98.94
	8.9 to 9.6	41.00	0.053	0.008	98.79
	9.6 to 10.3	36.17	0.131	0.024	97.03
	10.3 to 11	38.61	0.061	0.014	98.60
	11 to 11.7	39.94	0.042	0.010	99.03
	11.7 to 12.4	41.54	0.037	0.007	99.14
<b>8</b>	8.2 to 8.9	40.89	0.042	0.008	99.04
	8.9 to 9.6	43.92	0.056	0.004	98.72
	9.6 to 10.3	36.67	0.105	0.022	97.62
	10.3 to 11	39.49	0.039	0.011	99.11
	11 to 11.7	41.01	0.019	0.008	99.56
	11.7 to 12.4	41.09	0.026	0.008	99.40
<b>13</b>	8.2 to 8.9	38.38	0.013	0.015	99.70
	8.9 to 9.6	41.43	0.031	0.007	99.30
	9.6 to 10.3	41.62	0.032	0.007	99.26
	10.3 to 11	42.04	0.019	0.006	99.57
	11 to 11.7	43.32	0.013	0.005	99.70
	11.7 to 12.4	44.20	0.015	0.004	99.66

The analyses of the data allow concluding that with the increase of the carbonyl iron concentration, in a generalized way, decreases the portion of reflected energy on the nanofibers surfaces and increases the portion of transmitted energy. Also, similar behavior is observed for all concentrations, the peak of reflected energy is in the first interval of frequencies, with decrease until frequencies around 9.2 GHz and new gain of reflected energy in frequencies around 9.9 GHz, finally decreasing until 12.4 GHz. Meanwhile, in the transmission energy, a decrease is observed in frequencies around 9.9 GHz, which is associated with the increase of reflected energy in the same frequencies.

Despite the characteristics observed in the quantitative analysis of the data, the nanofibers are intrinsically transmitter of the microwaves in the X-band.

#### 4 Conclusion

Through electrospinning of the polymer solution of Polysulfone in N,N-Dimethylacetamide with the dispersion of the ferromagnetic additive carbonyl iron, nanofibers blankets were processed.

From the variation of the processing parameters: polymer concentration, applied voltage and working distance, together with the morphological analysis by SEM, the optimal processing parameters were determined, where it was observed a lower presence of defects and high homogeneity of the nanofibers. The nanofibers were processed with the dispersion of the additive in different concentrations, up to 13 %m/m.

With the electromagnetic characterization by means of the vector network analyzer and rectangular waveguide, it was determined the interaction of the electromagnetic waves, in the frequency range of 8.2 to 12.4 GHz of microwaves, with the nanofibers, characterizing the influence of the additive. The nanofibers behave as wave transmitter. There is a discrete in the quantities of transmitted energy and decrease on the reflected energy with the increase of the ferromagnetic additive concentrations applied in this study.

**Acknowledgments:** The authors are grateful to CAPES, CNPq, Laboratory of Images (LAIMat) of São Paulo State University (UNESP/FEG) and to the Laboratory of Electronic Warfare (LAB-GE) of the Technological Institute of Aeronautics (ITA).

#### References

1. Roy, R., Roy, R. A., Roy, D. M. (1986). Alternative perspectives on “quasicrystallinity”: non-uniformity and nanocomposites. *Materials Letters*, 4(8-9), 323-328.
2. Paul, D. R., Robeson, L. M. (2012). Polymer nanotechnology: Nanocomposites. *Polymer*, 49, 3187-3204.
3. Camargo, P. H. C., Satyanarayana, K. G., Wypych, F. (2009). Nanocomposites: synthesis, structure, properties and new application opportunities. *Materials Research*, 12(1), 1-39.
4. Anandhan, S., Bandyopadhyay, S. (2011). Polymer nanocomposites: from synthesis to applications. In: J. Cuppoletti (Ed.), *Nanocomposites and polymers with analytical methods* (pp. 3-28). InTech.
5. Bakir, M., Meyer, J. L., Economy, J., Jasiuk, I. (2017). Aromatic thermosetting copolyester nanocomposite foam: High thermal and mechanical performance lightweight structural materials. *Polymer*, 123, 311-320.
6. Suriani, A. B., Norhafizah, J., Mohamed, A., Mamat, M. H., Malek, M. F. (2016). Scaled-up prototype of carbon nanotube production system utilizing waste cooking palm oil precursor and its nanocomposite application as supercapacitor electrodes. *Journal of Materials Science: Materials in Electronics*, 27, 11599-11605.
7. Abbasi, A., Sardroodi, J. J. (2017). Density functional theory (DFT) study of O<sub>3</sub> molecules adsorbed on nitrogen-doped TiO/MoS<sub>2</sub> nanocomposites: applications to gas sensor devices. *Journal of the Iranian Chemical Society*, 14, 2615-2626.
8. Sookhakian, M., Basirun, W. J., Teridi, M. A. M., Mahmoudian, M. R., Azarang, M. et al. (2017). Prussian Blue-nitrogen graphene nanocomposite as hybrid electrode for energy storage applications. *Electrochimica Acta*, 230, 316-323.
9. Mouriño, V. (2016). Polymer nanocomposites for drug delivery applications in bone tissue regeneration. In: H. Liu (Ed.), *Nanocomposites for musculoskeletal tissue regeneration* (pp. 175-186). Woodhead Publishing, Oxford.
10. Sol, P., Martins, A., Reis, R. L., Neves, N. M. (2016). Advanced polymer composites and structures for bone and cartilage tissue engineering. In: H. Liu (Ed.), *Nanocomposites for musculoskeletal tissue regeneration* (pp. 123-142). Woodhead Publishing, Oxford.
11. Huang, Z. M., Zhang, Y. Z., Kotaki, M., Ramakrishna, S.: a review on polymer nanofibers by electrospinning and their applications in nanocomposites. *Composites Science and Technology*, 63, 2223-2253.
12. Greiner, A., Wendorff, J. H. (2007). Electrospinning: a fascinating method for the preparation of ultrathin fibers. *Angewandte Chemie International Edition*, 46, 5670-5703.
13. Doshi, J., Reneker, D. H. (1995). Electrospinning and applications of electrospun fibers. *Journal of Electrostatics*, 35(2-3), 151-160.
14. Xie, Y., Guan, Y., Kim, S. H., King, M. W. (2016). The mechanical performance of weft-knitted/electrospun bilayer small diameter vascular prostheses. *Journal of the Mechanical Behavior of Biomedical Materials*, 64, 410-418.



15. Goetz, L. A., Jalvo, B., Rosal, R., Mathew, A. P. (2016). Superhydrophilic anti-fouling electrospun cellulose acetate membranes coated with chitin nanocrystals for water filtration. *Journal of Membrane Science*, 510, 238-248.
16. Almuhammed, S., Bonne, M., Khenoussi, N., Brendle, J., Schacher, L. et al. (2016). Electrospinning composite nanofibers of polyacrylonitrile/synthetic Na-montmorillonite. *Journal of Industrial and Engineering Chemistry*, 35, 146-152.
17. Minden-Birkenmaier, B. A., Selders, G. S., Cherukuri, K., Bowlin, G. L. (2017). Electrospun fibers/branched-clusters as building units of tissue engineering. *Electrospinning*, 1(1), 111-121.
18. Reyes, C. G., Sharma, A., Lagerwall, J. P. F. (2016). Non-electronic gas sensors from electrospun mats of liquid crystal core fibres for detecting volatile organic compounds at room temperature. *Liquid Crystals*, 43(13-15), 1986-2001.
19. Hong, X., Chung, D. D. L. (2017). Carbon nanofiber mats for electromagnetic interference shielding. *Carbon*, 111, 529-537.
20. Liang, J., Wang, Y., Huang, Y., Ma, Y., Liu, Z. et al. (2009). Electromagnetic interference shielding of graphene/epoxy composites. *Carbon*, 47, 922-925.
21. Chung, D. D. L. (2012). Carbon Materials of structural self-sensing, electromagnetic shielding and thermal interfacing. *Carbon*, 50, 3342-3353.
22. Sudha, J. D., Sivakala, S., Prasanth, R., Reena, V. R., Nair, P. R. (2009). Development of electromagnetic shielding materials from the conductive blends of polyaniline and polyaniline-clay nanocomposite-EVA: preparation and properties. *Composites Science and Technology*, 69, 358-364.
23. Chung, D. D. L. (2001). Electromagnetic interference shielding effectiveness of carbon materials. *Carbon*, 39, 279-285.
24. Dhawan, S. K., Singh, N., Rodrigues, D. (2003). Electromagnetic shielding behavior of conducting polyaniline composites. *Science and technology of Advanced Materials*, 4, 105-113.
25. Ebeuwele, R. O. (2000). *Polymer science and technology*. CRC Press, Florida.
26. Joseph, N., Sebastian, M. T. (2013). Electromagnetic interference shielding nature of PVDF-carbonyl iron composites. *Materials Letter*, 90, 64-67.
27. Lee, S. M. (1991). *International encyclopedia of composites*. VCH Publishers, New York.